A COOLING RATE ANALYSIS IN THE GTA ALUMINUM ALLOY WELDING

Magalhães, E.S., Lima e Silva, A.L.F. and Lima e Silva, S.M.M.*.
*Author for correspondence
Heat Transfer Laboratory – LabTC,
Mechanical Engineering Institute - IEM,
Federal University of Itajubá - UNIFEI,
Av. BPS, 1303
Itajubá, MG, Brazil
E-mail: elisan@unifei.edu.br, alfsilva@unifei.edu.br, metrevel@unifei.edu.br

ABSTRACT

This work presents an analysis of the heat transfer by convection and radiation during a GTA (Gas Tungsten Arc) aluminum welding process. The authors in-house C++ previous developed code was modified to calculate the amount of heat transfer by convection and radiation. In this software, an iterative Broydon-Fletcher-Goldfarb-Shanno (BFGS) inverse method was applied to minimize the amount of heat delivered to the plate when the appropriate sensitivity criteria were defined. In the software, the thermal properties were considered temperature-dependent. The methodology was validated by accomplishing lab controlled experiments. In order to improve the study, four positive polarities conditions were tested during the lab experiments. Due to some experimental singularities, the forced thermal convection induced by electromagnetic field and thermal-capillarity force could be disregarded. Significant examples of these singularities are the relatively small weld bead when compared to the sample size and the reduced time of welding process. In order to evaluate the local Nusselt number, empirical correlations for flat plates was used. The Nusselt number was applied to estimate the local heat transfer coefficient *h*. The presented method solved the thermal problem satisfactorily. The numerical cooling rate analysis presented the same pattern for all experimental conditions. The Free Convection proves to be the dominant effect in the cooling rate after the welding torch is turned off. However, the thermal radiation emission plays a major role on the cooling process while the GTA torch is on. The thermal radiation emissivity reaches this peak at the end of the welding process. The study also found that the heat losses by convection and radiation of the weld pool do not affects significantly the cooling process.

INTRODUCTION

The GTA (Gas Tungsten Arc) welding process is largely used in industrial applications nowadays. Due to its great welding quality and low equipment cost, this process is extensively applied to stainless steel, titanium alloy and nonferrous metals welds [1]. In the GTA welding process, a tungsten electrode is protected by a flow of inert gas; argon is usually employed as well as helium, nitrogen, hydrogen or mixtures. The knowledge of the heat flux, temperature gradients and cooling process are thoroughly necessary for welding process studies. The thermal analysis is fundamentally based on

NOMENCLATURE

A_{xy}	[m^2]	Area where is applied the heat flux
C	[J/kgK]	Specific heat
f		Liquid fraction
H	[J/kg]	Enthalpy function
h	[W/m^{2}K]	Heat transfer coefficient
Gr		Grashof number
L	[J/kg]	Specific latent heat
Nu		Nusselt number
q	[W/m^2]	Heat flux distribution
Q	[W/m^2]	Heat input from BFGS
r	[m]	Radius
Ri		Richardson number
t	[K]	Temperature
t	[s]	Time
$t+$	[s]	Time that the electrode remains on positive polarity
u	[m/s]	Velocity on x direction
x	[m]	Cartesian axis direction
y	[m]	Cartesian axis direction
z	[m]	Cartesian axis direction

Special characters

λ	[W/mK]	Thermal conductivity
ε		Emissivity
ρ	[kg/m^3]	Density
η	[m]	Normal direction

Subscripts

m	Melting point
l	Local
∞	Environment

models of heat transfer theory, which includes the following phenomena: Specific Heat, Latent Heat, Two Phase Regions, Moving Interfaces, Conservation of Energy, Fluid Mechanics, Conductivity, Contact Resistance, Radiation Emissivity and Convection [2].

The weld quality depends on several parameters to control the temperature of the workpiece. For instance, the electric current and the torch speed are important factors of the GTA welding process [3-4]. The cooling rate is an important factor that affects all welding processes quality. This heat loss occurs due to the diffusion, free convection and radiation. Those effects occur spontaneously; therefore, it is difficult to control the cooling rate during the welding process. There are several ways to control the heat loss in a welding process; one of them is to control the heat diffusion on the workpiece by making a preheating of the sample [5]. Another one is making the process in a vacuum room, which will obliterate the free convection [6]. However, the thermal emission by radiation cannot be minimized. As the matter of fact, any matter with a temperature bigger than absolute zero will emit thermal radiation. This factor limits the thermal radiation control.

Several authors have been studying numerical models for welding process. Those models predict satisfactory the temperature at the peak point [7-8]. However, they fail on the cooling analysis because they use simple approaches for radiation emission and the heat transfer coefficient by convection. For instance, Gonçalves et al. [7] used a three dimensional model based on the diffusion equation and the enthalpy method to model a TIG welding process. The authors' model used an empirical correction to estimate the heat transfer coefficient on the sample. However, this model did not consider the thermal emission by radiation. Thus, as expected, the model fail in predict the temperature after the TIG weld torch is turned off. The same pattern could be seen in Aissani *et al*. [8]. In their work, the authors model a TIG welding process for the same stainless steel of Gonçalves *et al*. [7]. They used a linearization of the radiation equation of Stefan-Boltzmann law and a constant heat transfer coefficient for the convection analysis. Although the authors' model covers the radiation and the convection, the use of a linear approach in a welding model is not recommended due to the high thermal gradient characteristic of the process. The author's model predicts well the heating part of the problem; on the other hand, it fails on analysing the cooling part.

In a previous work Magalhães *et al.* [9], a numerical software, based on an inverse problem and enthalpy method, was developed in order to predict the thermal field on a GTA aluminium welding. The thermal field in any region of the plate or any time was determined through the numerical solution of the tree dimensional heat diffusion equation. The inverse technique of BFGS (Broydon-Fletcher-Goldfarb-Shanno) was used to minimized the heat input on the process. The Finite Difference Method and the Implicit Euler Method for time discretization was used to solve the heat diffusion equation.

Some improvements are made in relation to the previous work. In this work, a detailed analysis on the cooling process is presented. Furthermore, the heat losses are presented separately in two fronts: convection and radiation. It is also analysed the cooling influence of the weld pool during the welding process. The average heat transfer coefficient, h, and the average Nusselt, Nu, number are also presented as function of time and polarity. Moreover, the visual distribution of the h for one experimental conditions is presented.

MATHEMATICAL MODEL

Figure 1 describes the GTA welding problem. It consists of a GTA torch that applies a heat flux over an aluminum plate. This GTA torch follows the direction s, with a velocity u. This heat input will cause a thermal gradient on the plate which could be described by the heat diffusion equation. When the thermal field starts, a heat loss due to the spontaneous effects of convection and radiation begins.

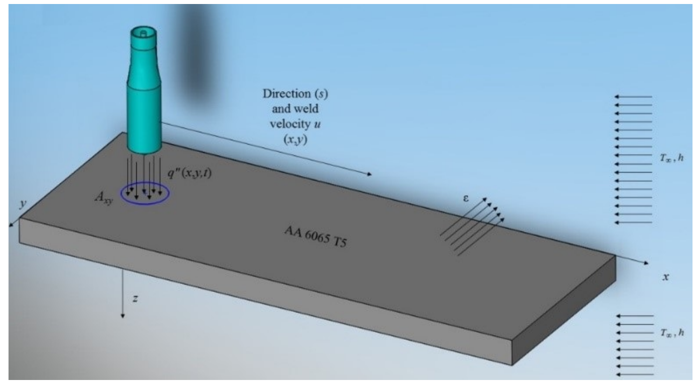

Figure 1 Scheme representation of the three-dimensional thermal welding process.

The GTA welding process may be expressed by the heat diffusion equation for space:

$$\frac{\partial}{\partial x}\left(\lambda(T)\frac{\partial T}{\partial x}\right)+\frac{\partial}{\partial y}\left(\lambda(T)\frac{\partial T}{\partial y}\right)+\frac{\partial}{\partial z}\left(\lambda(T)\frac{\partial T}{\partial z}\right) = \rho\frac{\partial H(T)}{\partial t}, \tag{1}$$

where x, y and z are the Cartesians coordinates, T the temperature, λ the thermal conductivity, ρ the density. The enthalpy function H is defined as:

$$H = \int C dT + fL \tag{2}$$

where C is the specific heat, L the latent heat and f is the Heaviside step function defined as function of the melting temperature, T_m:

$$\begin{aligned} f(T) &= 1 \qquad T > T_m \\ f(T) &= 0 \qquad T < T_m \end{aligned} \tag{3}$$

The problem analysed is subject to the boundary conditions of convection and radiation:

$$-\lambda(T)\frac{\partial T}{\partial \eta} = h(T)(T - T_\infty) + \sigma\varepsilon(T)\left(T^4 - T_\infty^4\right) \tag{4}$$

where η is the normal direction, h the heat transfer coefficient by convection, σ the Stefan-Boltzmann constant, ε the emissivity and T_∞ the room temperature.

The following boundary condition of heat flux, q", prescribed is applied to the area A_{xy}:

$$-\lambda(T)\frac{\partial T}{\partial z} = q''(x, y, t) \tag{5}$$

The initial condition of prescribed temperature is used for the entire domain as:

$$T(x, y, z, 0) = T_\infty \tag{6}$$

The solution of the temperature field is obtained through the numerical approximation of Eq. (1) by using Finite Difference method with implicit formulation on time. The linear system of algebraic equations is solved by using MSI (Modify Strongly Implicit) procedure [10].

The heat flux, $q(x,y,t)$ (see Fig. 1) is applied to a circular region with radius r and area A_{xy}. It has a Gaussian distribution and releases its energy continuously over the time as it moves with a constant velocity u positive in x direction [2]:

$$q(x,y,t)=\frac{3Q(t)}{\pi\times r^2}e^{-3\frac{(x-u)^2}{r^2}}e^{-\frac{3y^2}{r^2}} \tag{6}$$

where the $Q(t)$ is the minimized heat input function from the BFGS inverse technique [11].

Numerical Model

Due to the temperature gradients in the air and the gravitational field, there is an induction of natural convection currents around the sample. The Nusselt number obtained from empirical correlations of the literature [12] was used to determine the convection coefficient h.

The cooling rate analysis is based on the experimental procedure and data from [9]. In that work, four t+ experimental conditions (2ms, 7ms, 11ms and 13ms) were tested and three experiments were carried out for each condition with the aim of assessing the repeatability of the estimated heat flux results. Four experimental temperatures were used to estimate the heat flux by using the BFGS technique. The temperatures were collected from four thermocouples fixed on the opposite side of the weld region. For each experiment, 482 temperature points were observed at a time interval, Δt, of 0.78 s. The welding speed was 62.5 mm/min.

In the present work, the simulations were carried out using a new mesh to enhance the previous software [9]. The Cartesian mesh is non-uniform and it has an overall of 225.000 volumes. This mesh configuration maximizes the number of mesh points on the heated region (Figure 2) where the temperature gradients are higher. The melting temperature was delimited by the lowest temperature of solid-liquid transition, T_m = 615 °C [13]. The thermal properties as thermal conductivity, emissivity, thermal diffusivity, specific heat were taken from fitting data points of Jensen *et al*. [14]. For further details of the experimental procedure, experimental data and the methodology of the numerical code please see Magalhães *et al*. [9].

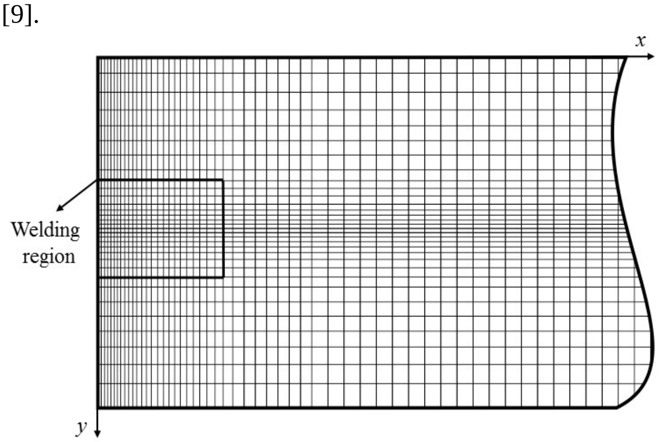

Figure 2 Non-uniform cartesian mesh applied in simulation (aerial view).

Numerical Analysis

The cooling analysis considered three conditions: the heat loss by convection and radiation on the Fusion Zone (FZ), the heat diffusion on the plate and the heat loss by convection and radiation of the heated plate. Figure 3 presents the schematic representation of the performed analysis. The blue colour represents the heat loss by convection and radiation on the FZ, the black arrows are the heat loss by convection and radiation on the sample.

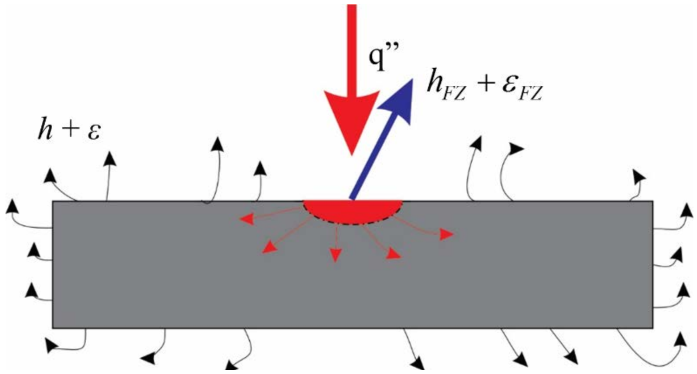

Figure 3 Scheme representation of the numerical performed analysis.

The presented work does not explore the influence of the heating and cooling rate on the microstructure of the FZ because it has been reported in another work of the authors [15].

RESULTS ANALYSIS

Figure 4 presents a comparison between the temperature signals measured by thermocouples T_1, T_2, T_3 and T_4. The respective numerical temperature was calculated from the C++ previous developed code [9] for the welding conditions t+ = 2ms, t+ = 7ms, t+ = 11ms and t+ = 13ms. It must be pointed out that the higher temperatures are obtained by the thermocouples after the GTA arch is turned off in t = 24ms.

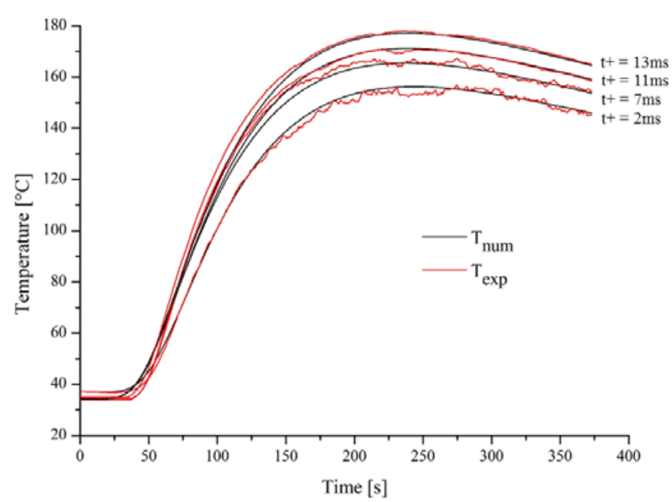

Figure 4 Evolution of the experimental and numerical temperatures for different t+ conditions.

From Figure 4, an increase in the temperature may be observed with the increase of positive polarity (t+). Theoretically, this temperature increase tends to decrease as the t+ exceeds 13ms. This could be explain due to that when the t+ grows, a bigger part of the heat generated by the voltaic arch remains on the electrode. This is undesirable for the process efficiency as also for the electrode lifespan [16].

The dimensionless Richardson number, $Ri = Gr_l / \mathrm{Re}_l^2$, remained much higher than one (Ri > 1000) in all calculated points; consequently, the problem could be treated as pure free convection [12]. Thus, the empirical correlations from Bergman *et al*. [12] were used to calculate Nu_l, local Nusselt number and h in any position on the plate.

Figure 5 presents the average Nu profile. The average Nusselt number is obtained from the arithmetic mean of all Nu_l on the surface of the plate. From the Figure 5 analysis, it could be noticed that the Nu grows on the first seconds of the process and it stabilizes until the arch torch is turned off. After the process, the average Nu starts to grow again. This behavior is due to the non-linear characteristics of the adopted thermal properties for air. It may also be noticed that the Nu is not sensible to the positive polarity. As the average temperature increases due to the positive polarity, the Nu number remains almost at the same value for all studied cases.

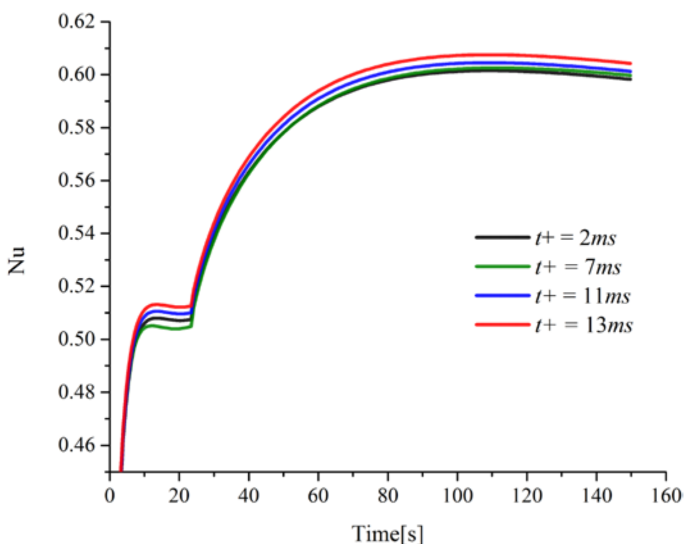

Figure 5 Average Nu on the plate as function of time.

Figure 6 shows the average heat transfer coefficient, h, for the four t+ welding conditions. It could be observed that the average heat transfer coefficient achieves the maximum value when the GTA torch is turned off. After this step of time, it starts to decrease slowly. The convection heat transfer coefficient will return to zero when the sample reaches the room temperature. It is also noticed that the convection heat transfer coefficient grows as the positive polarity increase. However, this increase of heat transfer by Free Convection as the positive polarity increases is not expressive. When all cases were compared, the heat transfer rate by convection had not grown more the 2W when we make the difference between t+ = 13ms and t+ = 2ms.

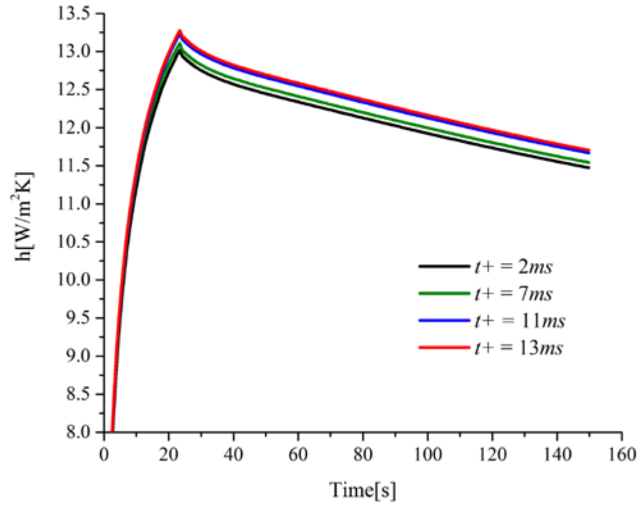

Figure 6 Heat transfer coefficient (h) as function of time.

The heat transfer rate lost by convection and radiation must be pointed out. As the heat transfer coefficient do not presented an expressive difference from one positive polarity to another (Figure 6), the Colling Rate presented almost the same values for all positive polarities conditions. Therefore, the cooling analysis were presented only for the t+ = 2ms experimental condition.

Figure 7 presents the heat loss by convection and radiation of the heated plate for the experimental condition t+ = 2ms. For this case, the estimate heat input from BFGS technique was 601W. Although the natural convection represents a big part of the overall cooling process, the heat loss by radiation affect significantly the cooling process while the GTA welding is performed. From the graphics analysis, the radiation emission reaches 311W in t = 24s while at the same point the heat loss by Free Convection is only 247W. However, the radiation emission decreases considerably when the TIG arch torch is turned off. For t = 140s the radiation emission is only 13W while the Free Convection is 53W.

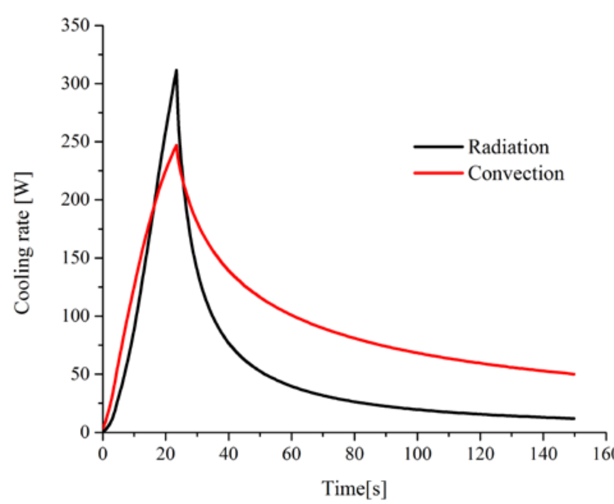

Figure 7 Heat transfer by Free Convection and Radiation for t+ = 2*ms*.

The Fusion Zone also loses heat by convection and radiation. However, those losses are not expressive when compared to the overall. Figure 8 presents a comparison between the heat loss by convection and radiation on the FZ. The melting point is reached when t = 3.9s. Before this point, the weld pool is not open. Thus, the thermal radiation emission and Free Convection of the weld pool is zero. After this point, both analyzed parameters starts to increase. Due to the higher temperature of the weld pool, the heat loss by radiation are more intense. However, those losses are not much expressive when it is compared to the heat losses of the plate. For instance, the higher radiation emission occurs when t = 24s. At this point GTA torch is turned off. It may be seen that at this instant the heat loss by radiation on the FZ reaches only 1.3W while the losses by Free Convection of the FZ are even more negligible, 0.3W. Therefore, the heat losses by convection and radiation are negligible to the process.

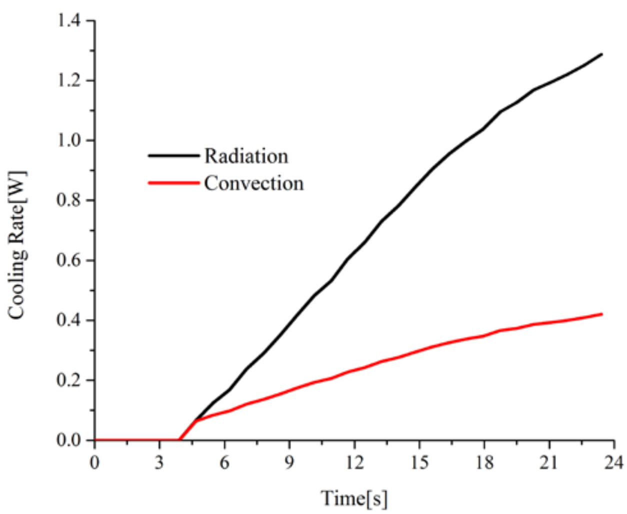

Figure 8 Heat losses on the Fusion Zone for $t+$ = 2ms.

Figures 9 presents the two-dimensional distribution of the heat transfer coefficient by convection for four time steps of the simulation of the welding condition $t+$ = 2ms. The Figure only presents the heated part of the sample. The distribution indicates that the highest value for the heat transfer coefficient, h, follows the GTA torch movement (Figure 9a and 9b). It may be seen that the convection coefficient reaches its highest value just before the torch is turned off (Figure 9c). After 24s, the heat transfer coefficient tends to decrease linearly until the sample reaches the room temperature and the heat transfer coefficient tends to zero (Figure 9d).

After the GTA torch is turned off, the heat input is finished. Thus, the diffused heat starts to be evenly distributed on the plate. Consequently, all surface points tend to have the same temperature and heat transfer coefficient.

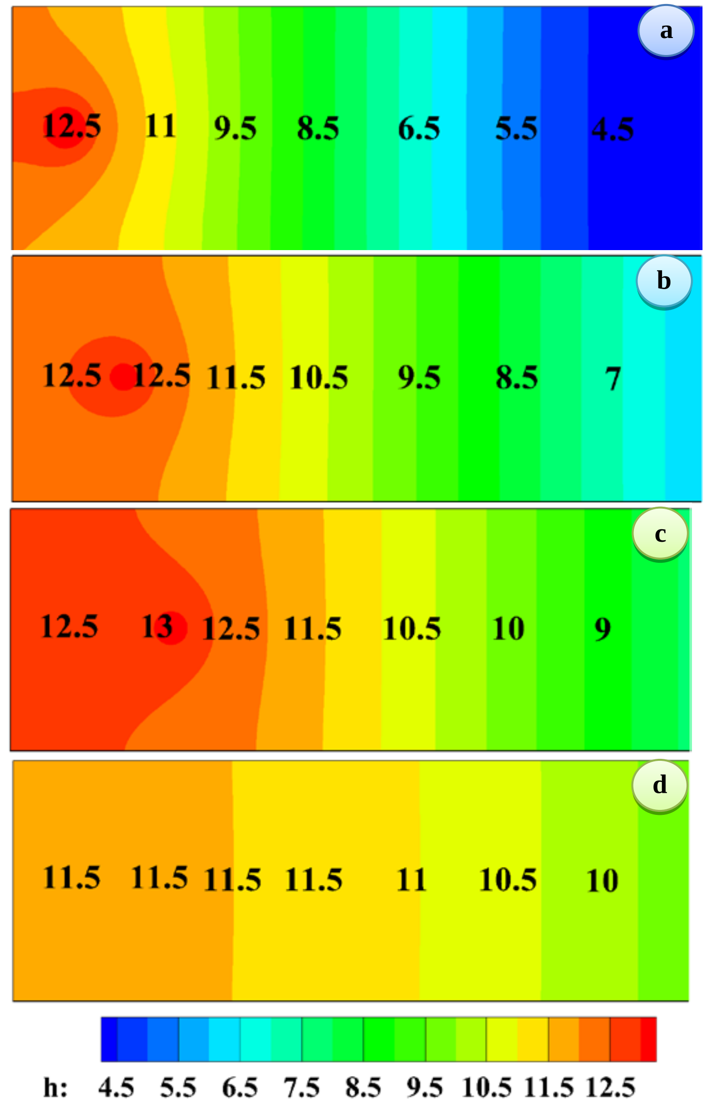

Figure 9 Evolution of the heat transfer coefficient, h [W/m^2K], at instants: a) 7.8s, b) 15.6s, c) 23.4s and d) 39.0s for $t+$ = 2.0ms.

The same visual disposition may be seen for the experimental condition $t+$ = 13ms. Likewise, the distribution indicates that the convection heat transfer coefficient reaches its maximum just under GTA torch. Figure 10 presents the visual approach for the heat transfer coefficient h.

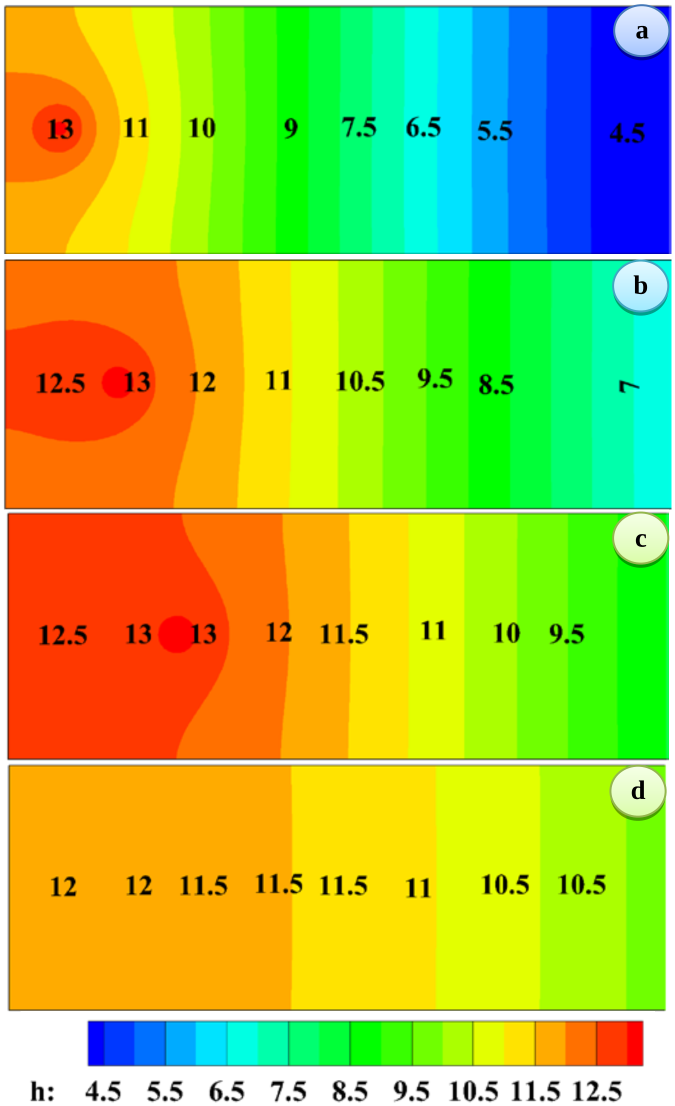

Figure 10 Evolution of the heat transfer coefficient, *h* [W/m^{2}K], at instants: a) 7.8s, b) 15.6s, c) 23.4s and d) 39.0s for t+ = 13.0ms.

CONCLUSION

This paper presented an analysis of the cooling rate (heat transfer rate lost) by convection and radiation on an aluminum 6065-T5 plate, under GTA welding process, from the observation of the thermal fields calculated by an in-house C++ code. The Free Convection effect is an important factor in heat transfer losses for the case analyzed. In fact, it is the prevailing effect a few seconds after the GTA torch is turned off. However, the radiation losses are significantly while the GTA torch stills on. The radiation emission reached 311W at the end of the welding process. The performed analysis represents an important step to improve the fusion and welding quality. The similarity between the experimental and calculated parameters validated and proved the efficiency of the software developed when applied to the resolution of thermal problems in welding.

ACKNOWLEDGMENTS

The authors thank the CNPq for its financial support and the master scholarship given to the student Elisan dos Santos Magalhães. The authors would also like to thank CAPES and FAPEMIG (Process APQ-0334-14) for their financial support.

REFERENCES

[1] Dong, W., Lu, S., Li, D. and Li, Y., GTAW liquid pool convections and the weld shape variations under helium gas shielding, *International Journal of Heat and Mass Transfer*, Vol. 54, 2011, pp. 1420-1431.

[2] Goldak, J.A. and Akhlaghi, M., Computational welding mechanics, *Springer*, 2005.

[3] Li, D., Lu, S., Dong, W., Li, D. and Li, Y., Study of the law between the weld pool shape variations with the welding parameters under two TIG process, *Journal of Materials Processing Technology*, Vol. 212, 2012, pp. 128-136.

[4] Yadaiah, N. and Bag, S., Effect of heat source parameters in thermal and mechanical analysis of linear GTA welding process, *ISIJ International*, Vol. 52, 2012, pp. 2069-2075.

[5] Zareie Rajani, H.R., Torkamani, H., Sharbati, and Raygan, Sh., Corrosion resistance improvement in Gas Tungsten Arc Welded 3316L stainless steel joints through controlled preheat treatment, *Materials and Desing*, Vol. 34, 2011, pp. 51-57.

[6] Radzievskii,V.N., Rymar, V.I., Besednyi, V.A., Chernov V.Yu.,Use of high-temperature vacuum welding in fabrication of the parts of centrifugal compressors, *Chemical and Petroleum Engineering*, Vol. 11, No. 10, 1975, pp.925-927.

[7] Gonçalves, C.V., Carvalho, S.R., Guimarães, G., Application of optimization techniques and the enthalpy method to solve a 3D-inverse problem during a TIG welding process, *Applied Thermal Engineering*, Vol. 30, 2010, 2396-2402.

[8] Aissani, M., Guessasma, S., Zitouni, A., Hamzaoui, R., Bassir, D., Benkedda, Y., Three-dimensional simulation of 304L steel TIG welding process: Contribution of the thermal flux, *Applied thermal Engineering*, Vol. 89, 2015, 822-832.

[9] Magalhães, E.S., Carvalho, S.R., Lima e Silva, A.L.F., Lima e Silva, S.M.M., The use of non-linear inverse problem and the enthalpy method in GTAW process of aluminum, *International Communications in Heat and Mass Transfer*, Vol. 66, 2015, pp. 114-121.

[10] Schneider, G.E. and Zenan, M., A Modified strongly implicit procedure for the numerical solution of field problems, *Numerical Heat Transfer*, Vol. 4, 1981, pp. 1-19.

[11] Vanderplaats, G.N., Numerical optimization techniques for engineering design, *McGraw Hill USA*, 4th ed., 2005, 465p.

[12] Bergman, T.L., Lavine, A.S., Incropera, F.P. and Dewitt, D.P., Fundamentals of Heat and Mass Transfer, *John Wiley & Sons*, 7th ed., 2011, USA, 1076p.

[13] Toten, E.F., and Macknzie, D.S., 2003. Handbook of Aluminum – Physical Metallurgy and Process, *Marcel Dekker Inc*, Vol. 1, 2003, 1309p.

[14] Jensen, J.E., Tuttle, W.A., Stwart, R.B., Brechna H., and Prodell, A.G., Selected Cryogenic Data Notebook, *Brookhaven National Laboratory*, United States Department of Energy, Vol. II, 1980.

[15] Magalhães, E.S., Correa, E.O., Lima e Silva, A.L.F., Lima e Silva, S.M.M., Microstrutural analysis in GTA aluminum alloy welding using inverse problems, *Applied Thermal Engineering*, Vol. 100, 2016, 333-339.

[16] Sarrafi, R. and Kovacevic, R., Chatodic cleaning of oxides from aluminum surface by variable-polarity arc, *Welding Journal*, Vol. 89, 2010, 1-10.